ADVANCED MATERIALS

DOI: 10.1002/adma.200700188

Assembly of Cobalt Phthalocyanine Stacks inside Carbon Nanotubes**

By *Karina Schulte*,* *Janine C. Swarbrick*, *Nicholas A. Smith*, *Federica Bondino*, *Elena Magnano*, and *Andrei N. Khlobystov*

Organic molecules are rapidly finding their way into electronic architectures and photovoltaic devices. In recent years a pronounced increase in efficiency has been achieved, which is largely due to the virtually unlimited tunability of the building blocks. Indeed, by selecting specific molecular structures and chemically optimizing their interaction with substrates and each other we can dramatically affect the macroscopic properties of novel assemblies. Metallo-organic molecules, like the phthalocyanines, are of particular interest as they can also carry localized magnetic moments.

Phthalocyanines are a class of stable, blue-green synthetic pigments which can be synthesized with a variety of metal ions at their center. They are related to the biologically important porphyrin family, which includes molecules like heme and chlorophyll. Within molecular nanotechnology their strong optical absorption is already being exploited in photovoltaic devices containing phthalo-fullerene mixed phases.[1] However, they also display other useful bulk optical properties including dichroism and luminescence,[2] and are used in gas-detection.[3] We have focused our experiments on cobalt phthalocyanine (CoPc) which consists of a planar carbon and nitrogen macrocycle with a single cobalt ion (see Fig. 1, inset). The cobalt ion has a partially filled 3d-orbital and is magnetically active.[4,5]

With this in mind, restricting phthalocyanine assemblies to one or two dimensions raises a variety of exciting issues as to what will happen to the electronic structure and hence to their optical, magnetic and transport properties. A particularly powerful method of forming one-dimensional molecular arrays is the encapsulation in a carbon nanotube.[6] The selection of carbon nanotubes as the container structures is motivated in part by the fact that nanotubes can act as a confining, as well as a shielding, environment.[7] Since we are dealing with planar molecules the precise internal stacking order will be important in assessing the physical properties of this assembly. Previously, planar molecules with a large aspect ratio, such as rectangular perylene-3,4,9,10-tetracarboxylic-3,4,9,10-dianhydride (PTCDA) have been shown to align virtually parallel to the nanotube axis,[8] whereas the elliptical fullerene C_{70} will align their long axis with the nanotube axis in narrow nanotubes (diameter 13.6 Å), but stand up in wider nanotubes (≥ 14.9 Å).[9,10] Magnetic effects have been observed recently in the encapsulation of azafullerene ($C_{59}N$).[11]

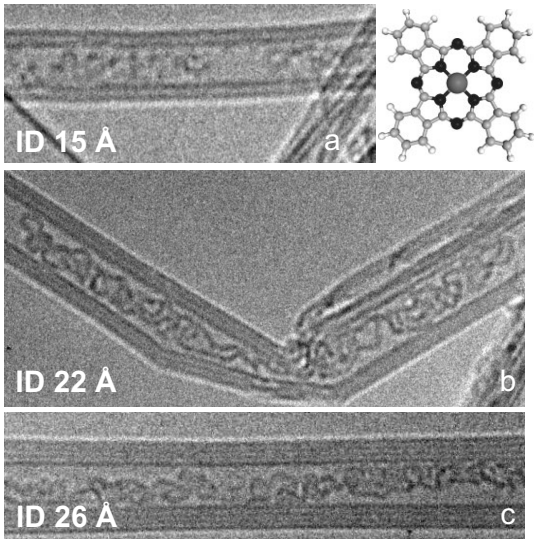

Figure 1. TEM images of CoPc filled nanotubes: a) The narrowest observed nanotube (15 Å inner diameter) filled with CoPc; b,c) Two multiwalled nanotubes showing a near optimal degree of filling. Note that all nanotubes have pristine surfaces. Inset: schematic drawing of a CoPc molecule, central ion: cobalt, black: nitrogen, grey: carbon, white: hydrogen.

Similarly, from the metallic point of view, both cobaltocene and ferrocene have been successfully encapsulated in nanotubes.[12,13] For both these molecules a strong interaction with the nanotubes is observed, resulting in electron doping of the nanotubes, which is confirmed by density functional calculations.[14]

Square planar CoPc occurs in two bulk forms.[15] The first one, α-CoPc, has a stacking angle $\gamma = 26°$ and is a metastable

[*] Dr. K. Schulte, Dr. J. C. Swarbrick, N. A. Smith
School of Physics and Astronomy, University of Nottingham
Nottingham NG7 2RD (UK)
E-mail: karina.schulte@nottingham.ac.uk
Dr. F. Bondino, Dr. E. Magnano
Laboratorio Nazionale TASC INFM-CNR
34012 Basovizza, Trieste (Italy)
Dr. A. N. Khlobystov
School of Chemistry, University of Nottingham
Nottingham NG7 2RD (UK)

[**] We gratefully acknowledge ELETTRA and the European Community for financial support under EU contract RII3-CT-2004-506008 (IA-SFS), and thank Prof. Phil Moriarty for valuable discussions. K.S. is supported by an Anne McLaren Fellowship from the University of Nottingham. A.N.K. is supported by the Royal Society, EPSRC and the European Science Foundation.

form, but can become energetically favoured below a critical volume.[16] The second bulk form, β-CoPc, is the stable phase and has a stacking angle $\gamma = 45°$. Measurements on thin films and monolayers of phthalocyanines on various substrates have found orientations varying smoothly from flat-lying molecules,[17,18] to α- and β-CoPc forms oriented with their stacking axis parallel to the surface depending on the particular substrate and growth parameters.[19–21]

In Figure 1 transmission electron microscopy (TEM) micrographs of selected individual nanotubes show the encapsulation of CoPc. Although the tubes are clearly filled, no obvious ordering of the encapsulated molecules could be observed in TEM. This could, however, be due to the fact that the intense electron beam used in TEM disturbs or even damages the CoPc molecules whilst imaging. Kataura et al. report similar problems employing TEM in imaging nanotube encapsulated Zn-diphenylporphyrins.[22] The narrowest filled nanotube observed is a double-walled carbon nanotube (DWCNT) with an inner diameter of 15 Å (see Fig. 1a). We can approximate the CoPc molecule by a square, with a planar van der Waals surface measuring 11×11 Å^2.[23,18] As the van der Waals radius of an sp^2-bonded carbon inside the nanotube wall is ~1.5 Å, this renders the nanotube with an effective inner van der Waals diameter of ~12 Å, which is smaller than the diagonal dimension of the CoPc molecule. In this case CoPc cannot enter the nanotube in a face-on configuration, and is constrained to angles ≤53° with respect to the nanotube axis in order to enter. Once inside, it also cannot flip to align with neighbouring CoPc molecules. In the larger diameter multiwalled carbon nanotubes (MWCNT), however, CoPc molecules can enter freely and subsequently form a lowest equilibrium ordering state with neighboring molecules. As a consequence larger filling densities were indeed observed (see Fig. 1b and c). It is also clear from these three TEM pictures that no remaining CoPc adheres to the outside of the nanotubes and we can therefore assume that our near-edge X-ray absorption fine structure (NEXAFS) signal, discussed below, stems solely from encapsulated molecules.

The morphology of the sample used for NEXAFS measurements was investigated by scanning electron microscopy (SEM), and the results are shown in Figure 2. The nanotubes are mostly aggregated together in large bundles and are subsequently deposited lying predominantly parallel to the substrate surface. The bundles themselves, however, are not aligned with respect to each other and therefore the nanotubes can be considered to have random azimuthal orientation in the deposition plane. Separate attempts to align filled nanotubes using electrophoresis or electrospray did not provide dense enough samples for NEXAFS measurements and no reliable N K-edge signal could be observed.[24,25]

The determination of molecular orientations on surfaces using NEXAFS with linearly polarized light is well established.[26] The theory is applicable

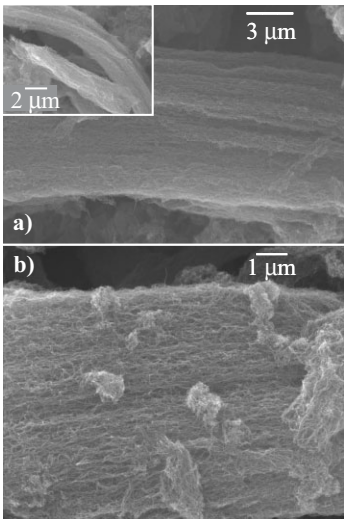

Figure 2. SEM images showing the arrangement of individual nanotubes in aligned bundles that lie predominantly parallel to the surface.

when localized electronic dipole resonances are excited by linearly polarized light near threshold. In organic molecules these resonances correspond to transitions from atomic 1s core levels into unoccupied π* or σ* levels which are highly localized on the individual molecules. For molecules with planar aromatic rings, like the phthalocyanines, the lowest unoccupied molecular orbital (LUMO) is a π* orbital formed by the antibonding combination of atomic p_z orbitals and is oriented perpendicular to the plane of the molecule. The dipole excitation from a spherically symmetric 1s level into the LUMO can therefore be represented by a vector $\vec{O}$, characterized by a polar angle v with respect to the surface normal, and an azimuthal angle ϕ defined by the projection of $\vec{O}$, onto the surface and the plane of X-ray incidence, spanned by the surface normal and the dominant electric field vector component $E_\parallel$ (the xz plane, see Fig. 3a). The incident light is character-

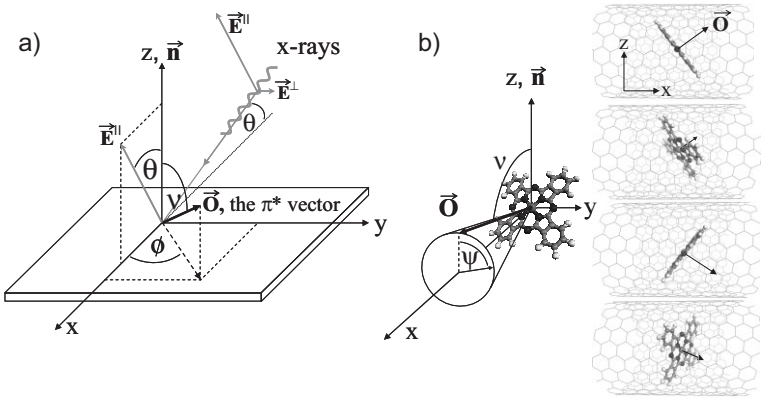

Figure 3. a) Coordinate system defining the used geometry in calculating the theoretical dependence of K-edge NEXAFS measurements (see text). The vector ***O*** is perpendicular to the CoPc molecular plane. b) Graphic depiction of the additional roll angle (Ψ) dependence necessary for describing nanotube-encapsulated molecules in NEXAFS.

ADVANCED MATERIALS

ized by an angle θ between $E_{\|}$ and the surface normal, or equivalently, by the angle between the substrate and the incoming X-ray beam. The resonance intensity is then given by:[26]

$$I^{\|} = A(\cos^2\theta\cos^2\nu + \sin^2\theta\sin^2\nu\cos^2\phi + 2\sin\nu\cos\nu\sin\theta\cos\theta\cos\phi) \quad (1)$$

$$I^{\perp} = A\sin^2\nu\sin^2\phi \quad (2)$$

$$I \propto PI^{\|} + (1-P)I^{\perp} \quad (3)$$

where A is the angle integrated cross section. The intensity $I^{\perp}$ arises from the minor electric field component perpendicular to the plane of X-ray incidence (along the y axis), in the case that the polarization factor P of the light is less than 1.

With nanotube-encapsulated molecules there is, however, another angle that needs to be considered. Even when the molecules inside are characterized by a fixed angle with respect to the nanotube axis, the nanotube itself can still sit in several "rolled" positions on the surface. This will also influence the measured value of ν as outlined in Figure 3b. With rotation around the z-axis contained in the azimuthal dependence we only need to consider the roll of a nanotube aligned along the x-axis. By introducing an angle Ψ (Fig. 3b), we can establish that the equations are modified in a way analogous to the azimuthal dependence, but now with a rotation around the x-axis:

$$I^{\|} = A(\cos^2\theta\cos^2\nu\,\mathbf{cos^2}\Psi + \sin^2\theta\sin^2\nu\cos^2\phi + 2\sin\nu\cos\nu\sin\theta\cos\theta\cos\phi\,\mathbf{cos}\Psi) \quad (4)$$

$$I^{\perp} = A\sin^2\nu\sin^2\phi\,\mathbf{sin^2}\Psi \quad (5)$$

We can then simplify these equations considerably, with added knowledge regarding the azimuthal and roll angles. The SEM images have established that the nanotubes lie predominantly parallel to the surface, but have, however, a random azimuthal angle. This is equivalent to a system with cylindrical symmetry around the z-axis and thus the equations can be simplified as done by Stöhr and Outka for threefold or higher symmetry, resulting in a replacement of $\cos^2\phi$ by its average 1/2 and $\cos\phi$ averaging to zero. Similarly, the random roll position of the nanotubes introduces a cylindrical symmetry around the x-axis with the same consequences for $\cos^2\Psi$ and $\cos\Psi$, giving (with $B = 1/2\ A$)

$$I^{\|} = B(\cos^2\theta\cos^2\nu + \sin^2\theta\sin^2\nu) \quad (6)$$

$$I^{\perp} = 1/2\ B\sin^2\nu \quad (7)$$

and the total intensity I as given before. By varying the angle θ of the incident X-rays, we can now extract a value for ν if the degree of polarization is known. From an angle dependent measurement of a monolayer of CoPc on silver terminated silicon obtained during the same beam time, we have established P to be 0.975 ± 0.005 over the N K-edge region.

The N K-edge NEXAFS spectra of CoPc filled multi-walled nanotubes are shown in Figure 4 for $\theta = 90°$ and $\theta = 28°$. In order to extract ν we have first normalised the raw spectra to the intensity profile of the incoming X-ray beam, I_0, measured simultaneously on a refocusing mirror mounted before the analysis chamber. This still left a linear slope which was subtracted by fitting a straight line through the low photon energy side of the spectra, before the onset of the π* resonance. The final step was done in three different ways: 1) normalizing the spectra to the high photon energy background; 2) normalizing to the integral under the curve from 395 to 420 eV; 3) normalization to the π*–σ* cross-over point at 405.2 eV. In each case measurements of the maximum intensity of the π* peak were taken, as well as the value of the integral from 395 eV to the cross-over point. These were then divided to give points that fall onto the theoretical curves, as plotted in Figure 5. The value for the angle ν between the vector perpendicular to the CoPc molecular plane and the surface normal is then read as $\nu = 54° \pm 5°$, which makes the stacking angle, inside the nanotube $\gamma = 36° \pm 5°$. Using our theoretical formula, a completely random distribution of stacking angles would yield $\nu = 45°$ and two identical N K-edge spectra. However, we do need to note this would be indistinguishable from a majority β-CoPc type filling, which also carries a stacking angle of 45°. Our measured stacking angle is exactly in between the two bulk form stacking angles of 26° (α-CoPc) and 45°, which could indicate that both stacking forms occur inside the nano-

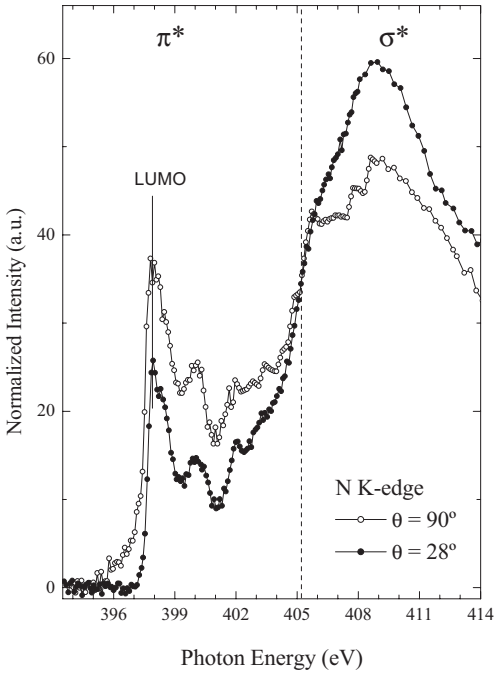

Figure 4. Nitrogen K-edge NEXAFS spectra showing the dependence of the π* and σ* intensity on the polar incidence angle θ of the light. The presented spectra have been normalized to coincide at the cross-over point between the π* and σ* regions (405.2 eV).

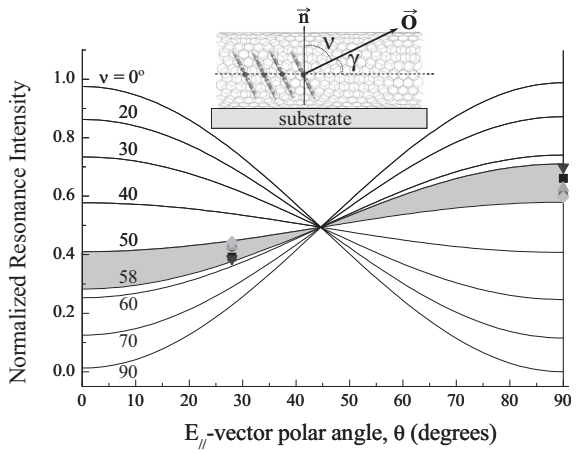

Figure 5. Normalized NEXAFS intensity at $\theta = 90°$ and 28° obtained from Fig. 4 in different ways (see text) and plotted onto the theoretical curves obtained with Eq. 6 giving an average value of $\nu = 54 \pm 5°$. Top: schematic drawing of encapsulated CoPc viewed side-on, defining the measured polar angle ν and internal stacking angle γ inside the nanotube.

tubes. If we, however, assume that a significant portion of the molecules is disordered this would have the effect of pushing the measured average angle ν closer to 45 degrees and in turn implying a stronger relative weight of the α-CoPc phase. Lastly, we cannot at this point control the spread in internal diameters of the nanotubes, which can also add to the preference of different internal phases and hence a spread in ν. Experiments with double-walled nanotubes of smaller diameter, and therefore a more forced type of filling, revealed too low a degree of filling to support trustworthy NEXAFS measurements. This mainly stems from the spread of internal diameters of double-walled nanotubes which is such that for an appreciable percentage of DWNTs filling cannot occur. This results in formation of "dilute" samples, i.e., mixtures of filled and empty nanotubes which cannot be separated, and therefore are difficult to characterize accurately by NEXAFS, as compared to multi-walled nanotubes.

In conclusion, we have presented the first example of encapsulation of metal-phthalocyanines in carbon nanotubes. No internal order could be discerned by TEM measurements, however, NEXAFS measurements reveal non-random stacking of the molecules inside the tube, characterised by a stacking angle $\gamma = 36° \pm 5°$. We believe this indicates a mixture of phases, coexisting in nanotubes, with a majority component possessing the α-CoPc ordering if we assume disorder in the film is significant. We would also like to note here that we have performed preliminary SQUID measurements on unaligned CoPc-containing nanotube samples, which suggest that there is a possible weak spin-glass transition occurring below 200 K (as evidenced by the difference between zero field cooled and field cooled runs). We are currently trying to solve practical problems and working towards advanced SQUID characterization of these materials which should provide additional information about their properties.

Experimental

Synthesis: Low residual catalyst, thin multi-walled carbon nanotubes (MWCNT) were obtained from Nanocyl. The tubes have an average number of layers between 3 and 6, and an average inner diameter of (24 ± 3) Å. Purified carbon nanotubes were first oxidized in air at 400 °C for 40 min, resulting in a weight loss of around 40 %. This thermal treatment opens the nanotube caps and also partly removes amorphous carbon from the surface of the tubes. They were then mixed with an excess of sublimation purified CoPc (Sigma-Aldrich) in a quartz tube, sealed in a vacuum of 10^{-6} Torr and heated at 375 °C for three days. CoPc that had settled on the outside of the nanotubes was successfully removed by repeated rinsing with a mixture of chloroform and 1 % trifluoroacetic acid. A small portion of the filled nanotubes was then dispersed onto a transmission electron microscopy (TEM) grid. Dried nanotubes were resuspended in methanol and sonicated for 30 min before being drop-deposited onto Si/SiO_2 substrates.

Transmission Electron Microscopy: TEM measurements were performed in a JEOL4000EX LaB6 microscope. In addition to the multi-walled nanotubes described above, a batch of double-walled carbon nanotubes (DWCNT), also from Nanocyl, with internal diameters ranging from 14–17 Å were filled in a similar way and used for the TEM studies only.

Near Edge X-ray Absorption Spectroscopy: The NEXAFS measurements were performed via Auger electron yield at the BACH beamline in Elettra with linear horizontal polarized light [27]. The beamline has an overall resolving power of 8000 around the nitrogen K-edge. The spot size at the sample was 15×300 μm^2. Photon calibration was established by measuring the well-known Si 2p core level in photoemission at various photon energies in the N K-edge range. All measurements were performed at room temperature.

Scanning Electron Microscopy: After the synchrotron measurements the morphology of the sample was checked in a JEOL JSM-7000F scanning electron microscope(SEM).

Received: January 22, 2007
Revised: April 3, 2007
Published online: September 21, 2007

[1] P. Peumans, A. R. Forrest, *Appl. Phys. Lett.* **2001**, *79*, 126.
[2] Y. Qiu, Y. D. Gao, P. Wei, L. D. Wang, *Appl. Phys. Lett.* **2002**, *80*, 2628.
[3] N. A. Rakow, K. S. Suslick, *Nature* **2000**, *406*, 710.
[4] A. R. Harutyunyan, A. A. Kuznetsov, O. A. Kuznetsov, O. L. Kaliya, *J. Magn. Magn. Mater.* **1999**, *194*, 16.
[5] A. Nath, N. Kopelev, S. D. Tyagi, V. Chechersky, Y. Wei, *Mater. Lett.* **1993**, *16*, 39.
[6] See a recent review: A. N. Khlobystov, D. A. Britz, G. A. D. Briggs, *Acc. Chem. Res.* **2005**, *38*, 901.
[7] D. A. Britz, A. N. Khlobystov, K. Porfyrakis, A. Ardavan, G. A. D. Briggs, *Chem. Commun.* **2005**, 37.
[8] Y. Fujita, S. Bandow, S. Iijima, *Chem. Phys. Lett.* **2005**, *413*, 410.
[9] A. N. Khlobystov, R. Scipioni, D. Nguyen-Manh, D. A. Britz, D. G. Pettifor, G. A. D. Briggs, S. G. Lyapin, A. Ardavan, R. J. Nicholas, *Appl. Phys. Lett.* **2004**, *84*, 792.
[10] L. H. Guan, H. J. Li, Z. J. Shi, L. P. You, Z. N. Gu, *Solid State Commun.* **2005**, *133*, 333.
[11] F. Simon, H. Kuzmany, B. Náfrádi, T. Fehér, L. Forró, F. Füllöp, A. Já nossy, L. Korecz, A. Rockenbauer, F. Hauke, A. Hirsch, *Phys. Rev. Lett.* **2006**, *97*, 136 801.
[12] L.-J. Li, A. N. Khlobystov, J. G. Wiltshire, G. A. D. Briggs, R. J. Nicholas, *Nat. Mater.* **2005**, *4*, 481.
[13] Y. F. Li, R. Hatakeyama, T. Kaneko, T. Izumida, T. Okada, T. Kato, *Nanotechnology* **2006**, *17*, 4143.
[14] V. M. García-Suárez, J. Ferrer, C. J. Lambert, *Phys. Rev. B* **2006**, *74*, 205 421.

[15] R. D. Gould, *Coord. Chem. Rev.* **1995**, *156*, 237.
[16] F. Iwatsu, *J. Phys. Chem.* **1988**, *92*, 1678.
[17] K. Kamiya, M. Momose, A. Kitamura, Y. Harada, N. Ueno, S. Hasegawa, T. Miyazaki, H. Inokuchi, S. Narioka, H. Ishii, K. Seki, *J. Electron Spectrosc. Relat. Phenom.* **1995**, *76*, 213.
[18] M. D. Upward, P. H. Beton, P. Moriarty, *Surf. Sci.* **1999**, *441*, 21.
[19] G. Dufour, C. Poncey, F. Rochet, H. Roulet, M. Sacchi, M. De Santis, M. De Crescenzi, *Surf. Sci.* **1994**, *319*, 251.
[20] L. Ottaviano, S. Di Nardo, L. Lozzi, M. Passacantando, P. Picozzi, S. Santucci, *Surf. Sci.* **1997**, *373*, 318.
[21] S. Kera, M. B. Casu, K. R. Bauchspieß, D. Batchelor, T. Schmidt, E. Umbach, *Surf. Sci.* **2006**, *600*, 1077.
[22] H. Kataura, Y. Maniwa, M. Abe, A. Fujiwara, T. Kodama, K. Kikuchi, H. Imahori, Y. Misaki, S. Suzuki, Y. Achiba, *Appl. Phys. A* **2002**, *74*, 349.
[23] B. Bialek, I. G. Kim, J. I. Lee, *Thin Solid Films* **2006**, *513*, 110.
[24] X. Q. Chen, T. Saito, H. Yamada, K. Matsushige, *Appl. Phys. Lett.* **2001**, *78*, 3714.
[25] J. N. O'Shea, J. B. Taylor, J. C. Swarbrick, G. Magnano, L. C. Mayor, K. Schulte, *Nanotechnology* **2007**, *18*, 035 707.
[26] J. Stöhr, D. A. Outka, *Phys. Rev. B* **1987**, *36*, 7891.
[27] M. Zangrando, M. Zacchigna, M. Finazzi, D. Cocco, R. Rochow, F. Parmigiani, *Rev. Sci. Instrum.* **2004**, *75*, 31.

